JOURNAL OF
Applied Polymer
SCIENCE

Special Issue: Polymers for Microelectronics

Guest Editors: Dr Brian Knapp (Promerus LLC) and
Prof. Paul A. Kohl (Georgia Institute of Technology)

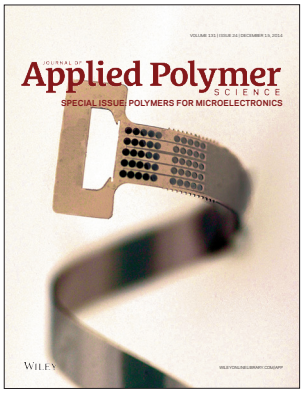

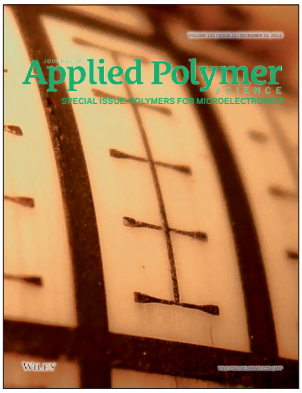

EDITORIAL

Polymers for Microelectronics
B. Knapp and P. A. Kohl, *J. Appl. Polym. Sci.* 2014, **DOI: 10.1002/app.41233**

REVIEW

Negative differential conductance materials for flexible electronics
A. Nogaret, *J. Appl. Polym. Sci.* 2014, **DOI: 10.1002/app.40169**

RESEARCH ARTICLES

Generic roll-to-roll compatible method for insolubilizing and stabilizing conjugated active layers based on low energy electron irradiation
M. Helgesen, J. E. Carlé, J. Helt-Hansen, A. Miller, and F. C. Krebs, *J. Appl. Polym. Sci.* 2014, **DOI: 10.1002/app.40795**

Selective etching of polylactic acid in poly(styrene)-block-poly(D,L)lactide diblock copolymer for nanoscale patterning
C. Cummins, P. Mokarian-Tabari, J. D. Holmes, and M. A. Morris, *J. Appl. Polym. Sci.* 2014, **DOI: 10.1002/app.40798**

Preparation and dielectric behavior of polyvinylidene fluoride composite filled with modified graphite nanoplatelet
P. Xie, Y. Li, and J. Qiu, *J. Appl. Polym. Sci.* 2014, **DOI: 10.1002/app.40229**

Design of a nanostructured electromagnetic polyaniline–Keggin iron–clay composite modified electrochemical sensor for the nanomolar detection of ascorbic acid
R. V. Lilly, S. J. Devaki, R. K. Narayanan, and N. K. Sadanandhan, *J. Appl. Polym. Sci.* 2014, **DOI: 10.1002/app.40936**

Synthesis and characterization of novel phosphorous-silicone-nitrogen flame retardant and evaluation of its flame retardancy for epoxy thermosets
Z.-S. Li, J.-G. Liu, T. Song, D.-X. Shen, and S.-Y. Yang, *J. Appl. Polym. Sci.* 2014, **DOI: 10.1002/app.40412**

Electrical percolation behavior and electromagnetic shielding effectiveness of polyimide nanocomposites filled with carbon nanofibers
L. Nayak, T. K. Chaki, and D. Khastgir, *J. Appl. Polym. Sci.* 2014, **DOI: 10.1002/app.40914**

Morphological influence of carbon modifiers on the electromagnetic shielding of their linear low density polyethylene composites
B. S. Villacorta and A. A. Ogale, *J. Appl. Polym. Sci.* 2014, **DOI: 10.1002/app.41055**

Electrical and EMI shielding characterization of multiwalled carbon nanotube/polystyrene composites
V. K. Sachdev, S. Bhattacharya, K. Patel, S. K. Sharma, N. C. Mehra, and R. P. Tandon, *J. Appl. Polym. Sci.* 2014, **DOI: 10.1002/app.40201**

Anomalous water absorption by microelectronic encapsulants due to hygrothermal-induced degradation
M. van Soestbergen and A. Mavinkurve, *J. Appl. Polym. Sci.* 2014, **DOI: 10.1002/app.41192**

Design of cyanate ester/azomethine/ZrO_2 nanocomposites high-k dielectric materials by single step sol-gel approach
M. Ariraman, R. Sasi Kumar and M. Alagar, *J. Appl. Polym. Sci.* 2014, **DOI: 10.1002/app.41097**

Furan/imide Diels–Alder polymers as dielectric materials
R. G. Lorenzini and G. A. Sotzing, *J. Appl. Polym. Sci.* 2014, **DOI: 10.1002/app.40179**

High dielectric constant polyimide derived from 5,5'-bis[(4-amino) phenoxy]-2,2'-bipyrimidine
X. Peng, Q. Wu, S. Jiang, M. Hanif, S. Chen, and H. Hou, *J. Appl. Polym. Sci.* 2014, **DOI: 10.1002/app.40828**

The influence of rigid and flexible monomers on the physical-chemical properties of polyimides
T. F. da Conceição and M. I. Felisberti, *J. Appl. Polym. Sci.* 2014, **DOI: 10.1002/app.40351**

JOURNAL OF
Applied Polymer
SCIENCE

Special Issue: Polymers for Microelectronics

Guest Editors: Dr Brian Knapp (Promerus LLC) and
Prof. Paul A. Kohl (Georgia Institute of Technology)

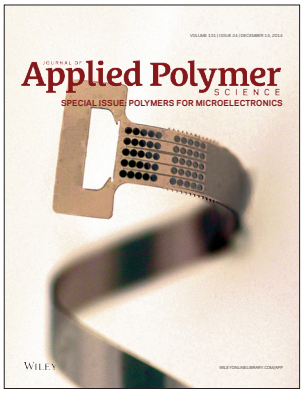

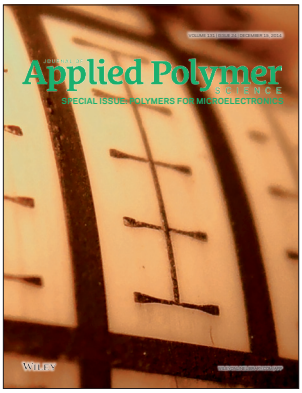

Development of polynorbornene as a structural material for microfluidics and flexible BioMEMS
A. E. Hess-Dunning, R. L. Smith, and C. A. Zorman, *J. Appl. Polym. Sci.* 2014, **DOI:** 10.1002/app.40969

A thin film encapsulation layer fabricated via initiated chemical vapor deposition and atomic layer deposition
B. J. Kim, D. H. Kim, S. Y. Kang, S. D. Ahn, and S. G. Im, *J. Appl. Polym. Sci.* 2014, **DOI:** 10.1002/app.40974

Surface relief gratings induced by pulsed laser irradiation in low glass-transition temperature azopolysiloxanes
V. Damian, E. Resmerita, I. Stoica, C. Ibanescu, L. Sacarescu, L. Rocha, and N. Hurduc, *J. Appl. Polym. Sci.* 2014, **DOI:** 10.1002/app.41015

Polymer-based route to ferroelectric lead strontium titanate thin films
M. Benkler, J. Hobmaier, U. Gleißner, A. Medesi, D. Hertkorn, and T. Hanemann, *J. Appl. Polym. Sci.* 2014, **DOI:** 10.1002/app.40901

The influence of dispersants that contain polyethylene oxide groups on the electrical resistivity of silver paste
T. H. Chiang, Y.-F. Chen, Y. C. Lin, and E. Y. Chen, *J. Appl. Polym. Sci.* 2014, **DOI:** 10.1002/app.41183

Quantitative investigation of the adhesion strength between an SU-8 photoresist and a metal substrate by scratch tests
X. Zhang, L. Du, and M. Zhao, *J. Appl. Polym. Sci.* 2014, **DOI:** 10.1002/app.41108

Thermodynamic and kinetic aspects of defectivity in directed self-assembly of cylinder-forming diblock copolymers in laterally confining thin channels
B. Kim, N. Laachi, K. T. Delaney, M. Carilli, E. J. Kramer, and G. H. Fredrickson, *J. Appl. Polym. Sci.* 2014, **DOI:** 10.1002/app.40790

Journal of Applied Polymer Science

Furan/Imide Diels–Alder Polymers as Dielectric Materials

Robert G. Lorenzini, Gregory A. Sotzing
Department of Chemistry & The Polymer Program, University of Connecticut, Storrs, Connecticut 06269
Correspondence to: G. A. Sotzing (E-mail: g.sotzing@uconn.edu)

ABSTRACT: Herein, the synthesis and characterization of a series of Diels–Alder (DA) polymers made with various bis-furans and 1,3-bis(maleimide)propane are described. Due to the fact that these syntheses produce no byproducts inherent to their mechanism, as well as the relative ease at which highly functionalized monomers can be made, these polymers are identified as candidates for dielectric materials with high dielectric constants. The dielectric spectra of these polymers are reported, with an emphasis placed on describing observed structure–property trends. Dielectric constants for these materials range from 4.31 to 6.75 at room temperature, with dielectric losses in the 1–2% regime. These polymers are thermally stable to ~130°C, where the retro DA reaction was confirmed with multiple analytical methods, including thermogravimetric analysis, differential scanning calorimetry, and gas chromatography/mass spectrometry thermal desorption spectroscopy. © 2013 Wiley Periodicals, Inc. J. Appl. Polym. Sci. **2014**, *131*, 40179.

KEYWORDS: addition polymerization; dielectric properties; structure–property relations

Received 4 September 2013; accepted 9 November 2013
DOI: 10.1002/app.40179

INTRODUCTION

The need for high-energy density dielectric materials is becoming more apparent as technological advancements continue to rapidly proceed. From the increase in demand for hybrid electric vehicles,[1] to the recent announcement by the US Navy to deploy the new "Laser Weapons System" (LaWS) onto the U.S.S. Ponce by 2014,[2] higher performing capacitors are required to bring these and other technologies into the next echelon. The current state-of-the-art for such capacitor materials is biaxially oriented polypropylene (BOPP), which has an operating temperature of 60–80°C,[3] a dielectric constant of ~2.2 at room temperature across a broad frequency range,[4] and a dielectric loss in the neighborhood of 10^{-3}–10^{-4}.[5]

Since the maximum energy density of a capacitor is directly proportional to its dielectric constant, the pursuit of materials with high dielectric constants is a good starting point toward high energy density capacitors. Currently, there are many teams working on high energy density dielectric materials. In terms of polymeric materials, efforts are focused in numerous areas including the functionalization of polypropylene,[6,7] polyvinylidene fluoride based composites,[8,9] and aromatic polyureas,[10] among others. Our group has previously published on polyureas and polyurethanes,[11] as well as on polyimides.[12]

Based on a series of calculations by members of our team,[11,13] it is known that electronegative species incorporated into the backbone of a polymer increases the dielectric constant. The bridging oxygen moiety inherent to the Diels–Alder (DA) adduct formed with maleimide and furan is an effective means of increasing the electronegativity of the backbone. In addition, the lack of byproducts inherent to the DA mechanism ensures high purity, which is crucial for electronic applications. DA reactions for both main chain polymers and crosslinking units are thoroughly described in the literature,[14–19] providing synthetic precedent and demonstrating the wide variety of possible functionalization. Most recently, furan-imide DA chemistry has been used in reversibly crosslinked self-healing networks,[20,21] and a thorough study on the reversibility of DA reactions has been published.[22] Of special importance for this application is the retro Diels–Alder temperature (rDA), as this will dictate the upper operating limit. In this work, a series of bis-furans are synthesized and polymerized with 1,3-bis(maleimide)propane (Figure 1), and the resulting polymers are characterized with time-domain dielectric spectroscopy (TDDS).

EXPERIMENTAL

Monomer Synthesis

The 1,3-bis(maleimide)propane common to the polymers has been synthesized by a modified procedure obtained from a European patent disclosure.[23] All of the following steps were executed in sealed vessels under N_2 atmosphere. Maleic anhydride (0.25 mol, Aldrich) was dissolved in dimethylformamide (DMF) (75 mL, Aldrich SureSeal™, anhydrous), and was cannulated into a flame-dried 250-mL 3-neck round bottom flask, equipped with a gas inlet, addition funnel, rubber stopper, and magnetic stirbar. 1,3-Diaminopropane (0.125 mol, Acros) was

© 2013 Wiley Periodicals, Inc.

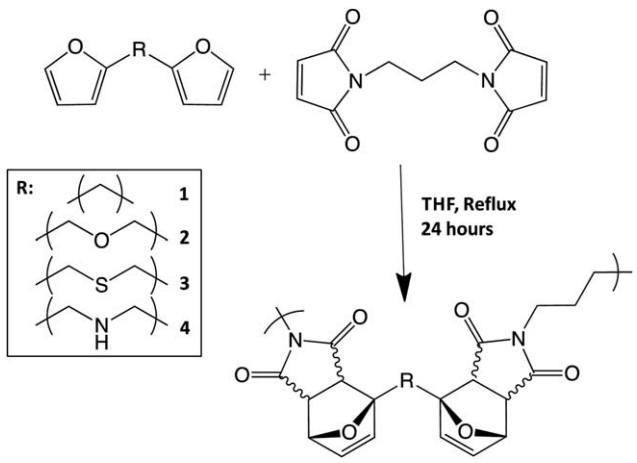

Figure 1. The maleimide-furan DA polymer with various functionalities.

dissolved in DMF (15 mL), and was cannulated into the addition funnel. The diaminopropane solution was added dropwise to the maleic anhydride solution for 1 h, and was stirred for an additional hour at 40°C. The formation of the amic acid upon mixing created a white, strand-like material that redissolved as stirring continued. Next, acetic anhydride (0.30 mol, Fisher) was added, followed by sodium carbonate (5.0 g, anhydrous, Fisher). This mixture was allowed to stir for 3 h at 40°C, after which it was cooled to room temperature, precipitated, and washed with ice-cold water and dried *in vacuo*. IR spectroscopy was used to confirm the absence of the broad amic acid peak at 3600–3300 cm^{-1}, ensuring full ring closure of the product. Yield = 76%, ^{1}H-NMR (400 MHz, $CDCl_3$, δ): 6.67 (4H, s), 3.51 (4H, t), 1.91 (2H, m).

2,2′-(Thiodimethylene)difuran was commercially available from Sigma Aldrich and was used as received.

The known 2,2′-methylenedifuran was prepared with furfuryl alcohol, furan, and trifluoroacetic acid as per the literature,[24] yield = 68%. ^{1}H-NMR ($CDCl_3$, δ) = 4.01 (2H, s), 6.09 (2H, m), 6.31 (2H, m), 7.33 (2H, m).

The known 2,2′-oxybis(methylene)difuran was synthesized as per the literature,[25] yield = 82%. ^{1}H-NMR ($CDCl_3$, δ) = 7.40 (2H, m), 6.34–6.31 (4H, m), 4.47 (4H, s).

N-((Furan-2-yl)methyl)furan-2-carboxamide[26]: It is important to note that this reaction is best done in open air, as large amounts of CO_2 are evolved. To a 500-mL round bottom flask was added a magnetic stirbar, furoic acid (35 mmol), and dichloromethane (150 mL). To this stirring solution was added 1,1′-carbonyl diimadazole (38.5 mmol), and after 45 min, furfuryl amine (38.5 mmol) was added. The mixture was allowed to stir overnight, after which it was quenched with 50 mL of 1*M* HCl. The mixture was transferred to a separatory funnel, and the aqueous layer was washed twice with dichloromethane (DCM). The combined organic layers were then washed with water (100 mL), brine (100 mL), and saturated sodium bicarbonate (100 mL). The solvent was removed via rotary evaporation, leaving behind a coarse white powder, 91% yield. ^{1}H-NMR ($CDCl_3$, δ) = 7.45–7.36 (2H, m), 7.16 (1H, m), 6.67 (1H, bs), 6.52 (1H, m), 6.36–6.32 (2H, m), 6.23 (2H, m).

The aforementioned amide was reduced with lithium aluminum hydride as per this procedure[21] to afford bis((furan-2-yl)methyl)amine, yield = 61%. The procedure was modified, heating the reaction mixture to reflux overnight instead of room temperature for 3 h. ^{1}H-NMR ($CDCl_3$, δ) = 7.39–7.37 (2H, m), 6.33–6.29 (4H, m), 3.84 (4H, s).

Polymer Synthesis

The polymer was synthesized via a modified procedure from the literature.[27] To a flame-dried 100-mL 3-neck flask equipped with a condenser, glass stoppers and a magnetic stirbar was added tetrahydrofuran (50 mL, ACS, Aldrich), the corresponding bis-furan (0.025 mol), and 1,3-bis(maleimide)propane (0.025 mol). The mixture was heated to reflux and stirred for 24 h under nitrogen atmosphere, after which the resultant polymer was precipitated in methanol, filtered, and refluxed in fresh methanol for 12 h. Finally, the polymer was filtered and dried overnight *in vacuo*. Yields for the polymerizations ranged from 64 to 78%. The resultant polymers were sparingly soluble in highly polar solvents, including DMF, dimethyl sulfoxide (DMSO), and dimethylacetamide (DMAc).

Characterization

^{1}H-NMR data was obtained on a Bruker DMX-500, using deuterated chloroform as the solvent. Gel permeation chromatography was conducted using dimethylacetamide as the mobile phase and polystyrene standards with the following instrumentation: Waters 515 HPLC pump, Waters 2414 refractive index detector, two mixed bed Jordi Gel DVB columns. Thermogravimetric analysis was conducted on a TA Instruments thermogravimetric analysis (TGA) Q500 by heating 10 °C/min from room temperature to 600°C in oxygen. Differential scanning calorimetry was performed on a TA Instruments differential scanning calorimetry (DSC) Q100: first, the sample was heated to 100°C at 10°C/min and was held isothermally for 5 min. It was then cooled to −50°C at 10°C/min. Data were obtained on the next cycle, when the sample was heated to 300°C at 10°C/min.

GC/MS Polymer Desorption Spectroscopy

Solid polymer sample was placed in a glass tube and was contained inside with a quartz wool plug. The tube was placed inside a custom-made sample holder,[28] which was dropped into the heating block of the injection port. Upon heating, desorbed materials were carried via helium into a capillary column, where they were fed into a Hewlett-Packard 6890 gas chromatography/mass spectrometry (GC/MS) system.

Film Preparation and TDDS Spectroscopy

Polymer films were drop cast on stainless steel shims from 5 wt % solutions prepared by heating and stirring in DMF, and were left on the bench overnight to allow a bit of solvent to evaporate off, leaving a "tacky" film; this step was crucial in making high-quality films. The samples were then heated in a vacuum oven at 75°C overnight to ensure complete removal of solvent, as confirmed by the aforementioned GC/MS polymer desorption method. Polymer films prepared in this way were determined to be 20–40 μm thick. Care was taken throughout to ensure the films were not contaminated with dust, etc. The dielectric spectra were obtained on an IMASS time domain dielectric spectrometer at the University of Connecticut

Table I. Physical Data for the Synthesized Polymers

Polymer	T_g (°C)	M_n (g mol^{-1})	M_w (g mol^{-1})	PDI	rDA by GC/MS (°C)	rDA by TGA (°C)	rDA by DSC (°C)
1	N/O	3650	8930	2.45	100	105	122
2	54	4540	10490	2.31	140	145	161
3	78	5660	9750	1.72	130	118	118
4	76	2920	8060	2.76	130	140	123

N/O = not observed.

Electrical Insulation Research Center. Measurements were taken at room temperature, 50°C, and 75°C between silicone rubber guarded electrodes.

RESULTS AND DISCUSSION

Gel Permeation Chromatography

The molecular weight data of the polymers are presented in Table I. The polymers show fairly low polydispersities, likely due to the solvent choice and workup conditions—the polymer chains reached a maximum length before becoming insoluble in tetrahydrofuran (THF), and refluxing in methanol removed some of the lower weight components. These data are consistent with similar polymers, as per the literature.[29] No significant change in the M_w was observed across bisfurans; however, the M_n of **4** is less than the rest of the polymers. The decrease in electronegativity of the amine moiety compared to an ether or thioether likely makes this monomer less reactive; electronegative substituents on the diene help to narrow the highest occupied molecular orbital/lowest unoccupied molecular orbital (HOMO/LUMO) gap between the diene and dienophile.

Thermal Data, rDA

Table I also presents the results from the various methods of probing the rDA temperature. It has been reported that the furan-imide DA adduct begins to rDA upwards of 80°C, depending on the substituents,[30] and our results are consistent with this finding. In the GC/MS method, polymer samples were heated in the injection port of the instrument between 100°C and 140°C in 10°C intervals; the presence or absence of volatile furan monomer peaks in the spectra indicated the onset of the rDA. In the TGA method, the rDA temperature was determined by the temperature at 1% weight loss, assuming that the weight loss was due to volatile monomer evaporating away after the onset of the rDA reaction. In the DSC method, the rDA temperature was elucidated from the onset of the peak resultant from the endothermic nature of the rDA.[25] All of the polymers except **4** showed a melting peak that overlapped with the rDA endotherm. The T_g exists within the measuring range of the TDDS, which explains the sharp increase in dielectric loss with respect to temperature, especially for **2**, which was immeasurable at 75°C due to high conductivity; the polymer was no longer an insulator. In all cases, the rDA is higher than the operating temperature of BOPP; therefore the rDA reaction is not a deterrent to using these materials in dielectric applications.

Dielectric Spectroscopy, Structure–Property Relationship

The dielectric data for each of the polymers at different temperatures are shown (Figures 2–5), along with the combined dielectric data of all the polymers at room temperature (Figure 6). The observed trend for dielectric constant is **3** > **2** > **4** > **1**. Our data show that the inclusion of an electronegative atom into the polymer backbone increases the dielectric constant. Based solely on electronegativity (increasing the polarizability inherent to the polymer), **2** should have the highest dielectric constant. Deviations from this trend are explained by the macromolecular polarization, or the alignment of dipoles while an electric field is applied.[31,32] The dielectric loss, however, follows the electronegativity trend at lower frequencies at room temperature. The polymers show a dispersion peak between 1 kHz and 10 kHz, which arises due to segmental motion in the polymer chains.[33] This is likely due to the two distinct portions of the polymer—the "hard" portion of the DA adduct combined with the "soft" linker units which are afforded some rotational degrees of freedom. Three of the polymers can be successfully measured at 75°C, whereas the other is measurable up to 50°C; these temperatures are toward the upper end of BOPP's operating range.

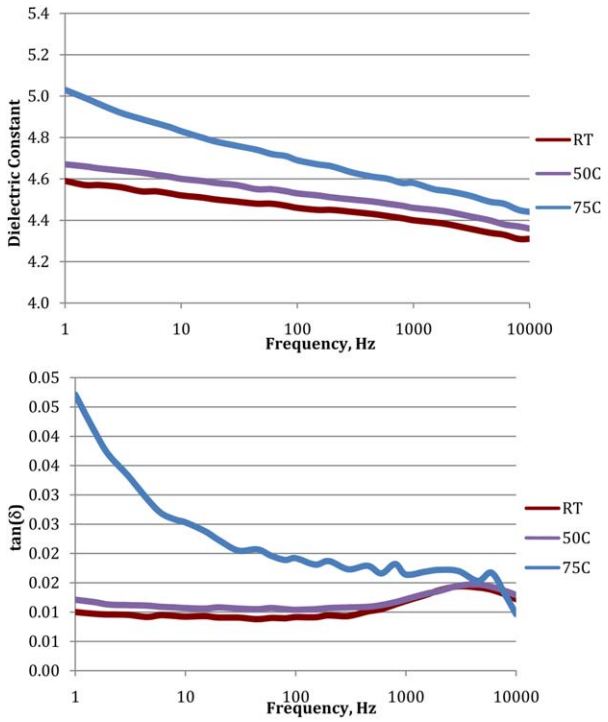

Figure 2. Dielectric spectrum (top) and dielectric loss (bottom) for polymer **1**. [Color figure can be viewed in the online issue, which is available at wileyonlinelibrary.com.]

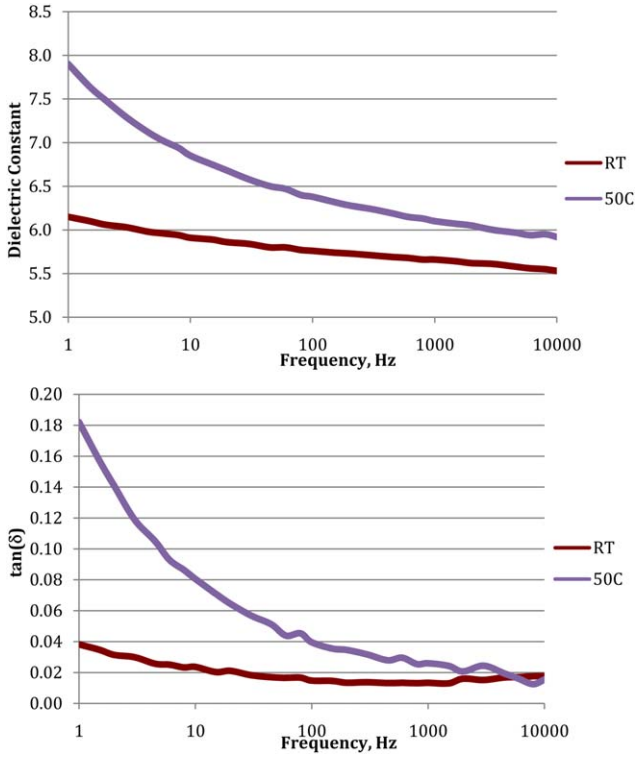

Figure 3. Dielectric spectrum (top) and dielectric loss (bottom) for polymer **2**. [Color figure can be viewed in the online issue, which is available at wileyonlinelibrary.com.]

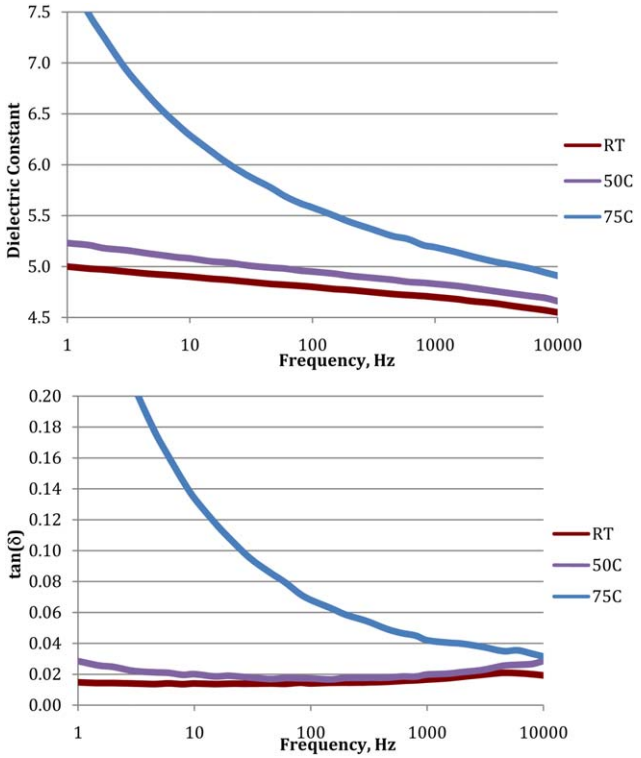

Figure 5. Dielectric spectrum (top) and dielectric loss (bottom) for polymer **4**. [Color figure can be viewed in the online issue, which is available at wileyonlinelibrary.com.]

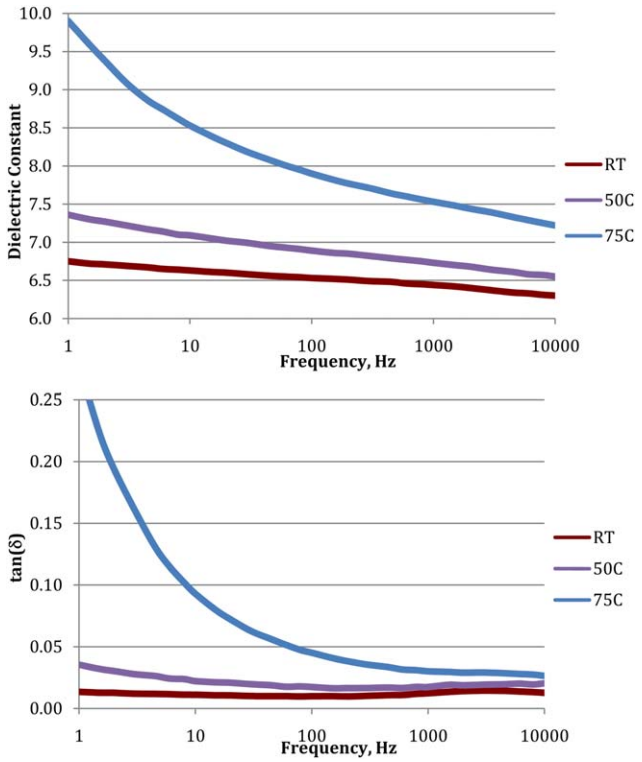

Figure 4. Dielectric spectrum (top) and dielectric loss (bottom) for polymer **3**. [Color figure can be viewed in the online issue, which is available at wileyonlinelibrary.com.]

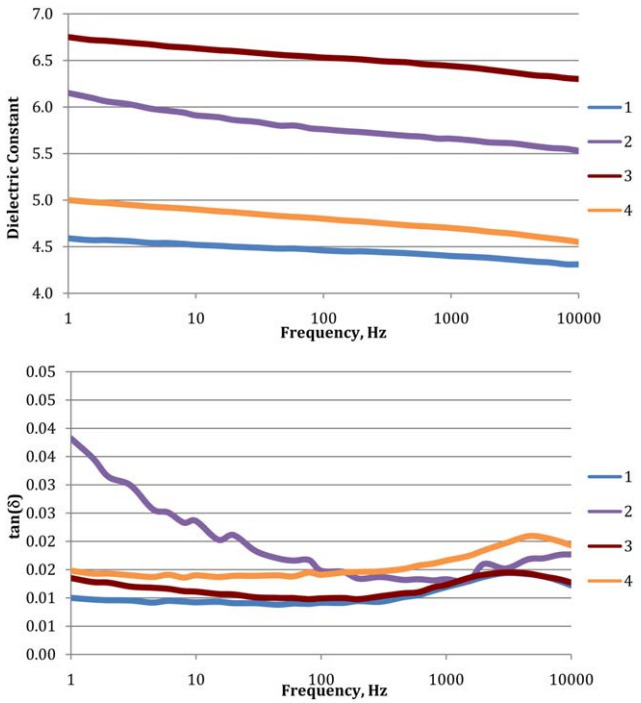

Figure 6. Overlaid dielectric spectra and dielectric loss of the polymers at room temperature. [Color figure can be viewed in the online issue, which is available at wileyonlinelibrary.com.]

CONCLUSIONS

In all cases, the synthesized polymers had dielectric constants exceeding that of BOPP, the current industry standard. Dielectric constants for the polymers ranged from 4.31 to 6.75 at room temperature, and dielectric losses were between 1 and 2% above 10 Hz. Increasing the electronegativity of the polymer backbone increased the dielectric constants in the following order: **3** > **2** > **4** > **1**. We have also demonstrated that the rDA is not a limiting factor for dielectric material applications based on current operating temperature standards. When designing these experiments, we hoped to both broadly span the chemical space looking for promising materials, as well as test the effect of electronegative substituents in the polymer backbone on the dielectric constant, and we consider these data to be successful toward our goal. We will continue to feed our dielectric results into a quantitative structure activity relationship, to be published at a later date, in the hopes of finding the best computational descriptors for increasing the dielectric constant.

ACKNOWLEDGMENTS

Authors acknowledge Ms. JoAnne Ronzello of the UConn Electrical Insulation Research Center for the dielectric measurements, and Dr. Ramamurthy Ramprasad for helpful discussions throughout. They are also grateful to the funding source, the Office of Naval Research through the Multi-University Research Initiative (MURI).

REFERENCES

1. Wouk, V. *Sci. Am.* **1997**, *227*, 70.
2. Osborn, K. Navy set to deploy rail guns, laser prototypes. Available at: http://www.dodbuzz.com/2013/04/29/navy-set-to-deploy-rail-guns-laser-prototypes/, DoD Buzz. Accessed 20 November 2013.
3. Zou, C.; Zhang, Q.; Zhang, S.; Kushner, D.; Zhou, X.; Bernard, R.; et al. *J. Vac. Sci. Technol.* B **2011**, *29*, 061401.
4. Anderson, E. W.; McCall, D. W. *J. Polym. Sci. Part A: Polym. Chem.* **1958**, *31*, 241.
5. Ho, J.; Jow, R. *Army Res. Lab.* **2009**, ARL-TR-4880.
6. Chung, T. C. M. *Green Sustainable Chem.* **2012**, *2*, 29.
7. Wang, C. C.; Pilania, G.; Ramprasad, R.; Agarwal, M.; Misra, M.; Kumar, S.; Yuan,, X.; Chung, T. C. M. *Appl. Phys. Lett.* **2013**, *102*, 152901.
8. Bhadra, D.; Masud, M. G.; Sarkar, S.; Sannigrahi, J.; De, S. K.; Chaudhuri, B. K. *J. Polym. Sci. Part B: Polym. Phys.* **2012**, *50*, 572.
9. Wang, Y.; Zhou, X.; Chen, Q.; Chu, B.; Zhang, Q. M. *IEEE Trans. Dielectr. Electr. Insul.* **2010**, *17*, 1036.
10. Wang, Y.; Zhou. X.; Lin. M.; Zhang, Q. M. *Appl. Phys. Lett.* **2009**, *94*, 202905.
11. Lorenzini, R. G.; Kline, W. M.; Wang, C. C.; Ramprasad, R.; Sotzing, G. A. *Polymer* **2013**, *54*, 3529.
12. Baldwin, A. F.; Ma, R.; Wang, C. C.; Ramprasad, R. Sotzing, G. A. *J. Appl. Polym. Sci.* **2013**, *130*, 1276.
13. Pilania, G.; Wang, C. C.; Wu, K.; Sukumar, N.; Breneman, C.; Sotzing, G.; Ramprasad, R. *J. Chem. Inf. Model.* **2013**, *53*, 879.
14. Kamahori, K.; Tada, S.; Ito, K.; Itsuno, S. *Macromolecules* **1999**, *32*, 3, 541.
15. Gandini, A. *Polímeros Ciência e Tecnologia* **2005**, *15*, 2, 95.
16. Grigoras, M.; Sava, M.; Colotin, G.; Simionescu, C. I. *J. Appl. Polym. Sci.* **2008**, *107*, 846.
17. Boutelle, R. C.; Northrop, B. H. *J. Org. Chem.* **2011**, *76*, 7994.
18. Bergman, S. B.; Wudl, F. *J. Mater. Chem.* **2008**, *18*, 41.
19. Shibata, M.; Asano, M. *J. Appl. Polym. Sci.* **2013**, *129*, 301.
20. Mallek, H.; Jegat, C.; Mignard, N.; Abid, M.; Abid, S.; Taha, M. *J. Appl. Polym. Sci.* **2013**, *129*, 954.
21. Zeng, C.; Seino, H.; Ren, J.; Hatanaka, K.; Yoshie, N. *Polymer* **2013**, *54*, 5351.
22. Mayo, J. D.; Adronov, A. *J. Polym. Sci. Part A: Polym. Chem.* **2013**, *51*, 5056.
23. Lancaster, M. BP Chemicals Limited. Eur. Pat. Appl.: 89311339.9 (**1989**).
24. Schwenter, M. E.; Vogel, P. *Chem.—Eur. J.* **2000**, *6*, 22, 4091.
25. Lautens, M.; Fillion E. *J. Org. Chem.* **1997**, *62*, 4418.
26. Kelly, C. B. Chemspider Synthetic Page 571 DOI: 10.1039/SP571
27. Gousse, C.; Gandini, A. *Polym. Int.* **1999**, *48*, 723.
28. Schematic courtesy of Gary Lavigne, www.syringeless.com
29. Canadell, J.; Fischer, H.; De With, G.; Van Benthem, R. A. T. M. *J. Polym. Sci. Part A: Polym. Chem.* **2010**, *48*, 3456.
30. Günay, K. A.; Theato, P.; Klok, H.-A. In Functional Polymers by Post-Polymerization Modification: Concepts, Guidelines, and Applications; Gevrek, T. N.; Arslan, M.; Sanyal, A., Eds.; Wiley-VCH Verlag GmbH & Co. KGaA, Weinheim, Germany, **2012**; p. 129.
31. Nunez-Regueira, L.; Gracia-Fernandez, C. A.; Gomez-Barreiro, S. *Polymer* **2005**, *46*, 5979.
32. Ben Amor, I.; Rekik, H.; Kaddami, H.; Raihane, M.; Arous, M.; Kallel, A. *J. Electrostat.* **2009**, *67*, 717.
33. Watanabe, H. *Macromol. Rapid Commun.* **2001**, *22*, 3, 127.